

AD-A131 393

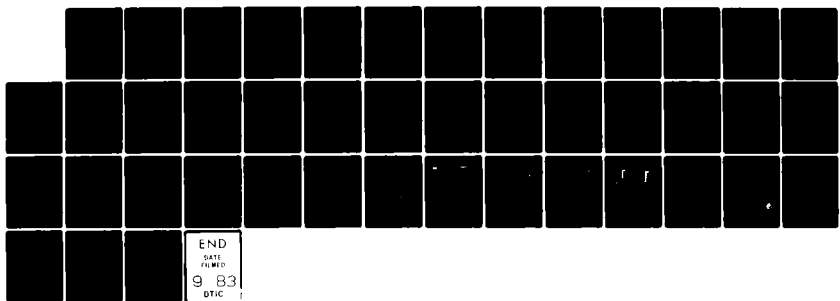
YIELD SURFACE FOR BARS INCLUDING WARPING RESTRAINT(U)  
WEIDLINGER ASSOCIATES NEW YORK R P DADDAZIO ET AL.  
01 FEB 82 DNA-TR-81-121 DNA001-81-C-0048

1//

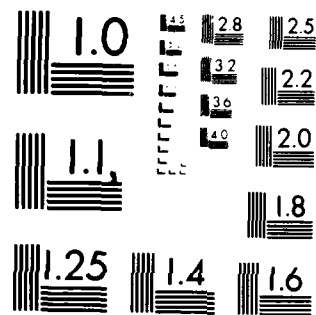
F/G 11/4

NL

UNCLASSIFIED



END  
DATE  
PRINTED  
9-83  
DTIC



MICROCOPY RESOLUTION TEST CHART  
NATIONAL BUREAU OF STANDARDS 1964

ADA131393

(12)

DNA-TR-81-121

## YIELD SURFACE FOR BARS INCLUDING WARPING RESTRAINT

Weidlinger Associates  
333 Seventh Avenue  
New York, New York 10001

1 February 1982

Technical Report

CONTRACT No. DNA 001-81-C-0048

APPROVED FOR PUBLIC RELEASE;  
DISTRIBUTION UNLIMITED.

THIS WORK WAS SPONSORED BY THE DEFENSE NUCLEAR AGENCY  
UNDER RDT&E RMSS CODE B344081466 Y99QAXSF00002 H2590D.

DTIC FILE COPY

Prepared for  
Director  
DEFENSE NUCLEAR AGENCY  
Washington, DC 20305

DTIC  
ELECTE  
S D  
AUG 15 1983  
B

83 07 18 045

Destroy this report when it is no longer  
needed. Do not return to sender.

PLEASE NOTIFY THE DEFENSE NUCLEAR AGENCY,  
ATTN: STTI, WASHINGTON, D.C. 20305, IF  
YOUR ADDRESS IS INCORRECT, IF YOU WISH TO  
BE DELETED FROM THE DISTRIBUTION LIST, OR  
IF THE ADDRESSEE IS NO LONGER EMPLOYED BY  
YOUR ORGANIZATION.



**UNCLASSIFIED**

**SECURITY CLASSIFICATION OF THIS PAGE (When Data Entered)**

**UNCLASSIFIED**

SECURITY CLASSIFICATION OF THIS PAGE(When Data Entered)

**20. ABSTRACT (Continued)**

furnishing the correct yield surface within the limits of validity of the assumptions made. The applicability and accuracy of the proposed equations are indicated.

**UNCLASSIFIED**

SECURITY CLASSIFICATION OF THIS PAGE(When Data Entered)

**PREFACE**

The authors would like to thank Professor Atle Gjelsvik for his gracious assistance and numerous suggestions during the course of this work.

Classified References, Distribution Unlimited  
No change per Mrs. Melanie Newlon, DNA/TIIM

Classification	U
Avail to other agencies	Yes
Attic	No
Dist	Specified
A	



TABLE OF CONTENTS

	<u>Page</u>
PREFACE . . . . .	1
LIST OF ILLUSTRATIONS . . . . .	3
INTRODUCTION . . . . .	5
KINEMATICS OF THIN WALLED OPEN CROSS SECTIONS . . . . .	7
DECOUPLING OF THE MIXED TORSION PROBLEM . . . . .	9
PLASTIC BEHAVIOR. . . . .	11
DETERMINATION OF A LOWER BOUND YIELD SURFACE. . . . .	13
DETERMINATION OF UPPER BOUND - YIELD MECHANISMS - UNIQUENESS. .	17
ACCURACY AND IMPLEMENTATION OF THE PROPOSED FORMULATION . . . .	20
CONCLUSION . . . . .	21
REFERENCES. . . . .	22
NOTATION . . . . .	24

LIST OF ILLUSTRATIONS

<u>Figure</u>		<u>Page</u>
1	Cross Section Displacements.....	28
2	Stress Components.....	28
3	Stress Resultants....	29
4	Z Stiffened Cylindrical Shell.....	30
5	Assumed Normal Stress Distributions.....	31
6	Z Section.....	31
7	Yield Surface Equations.....	32
8	Yield Surface Equations.....	33
9	Assumed Stress Distribution for Surface Element 1.....	34
10	Assumed Stress Distribution for Surface Element 2.....	34
11	Z Section Yield Surface.....	34
12	Z Section Yield Surface.....	35
13	Z Section Yield Surface.....	36

## INTRODUCTION

In recent years, considerable progress has been made in the development of computer programs to perform dynamic, large deflection, elasto-plastic analysis of submarine structures (1, 2, 3). A typical problem of interest is the dynamic elasto-plastic analysis of submerged, stiffened cylinders. Stiffeners on such cylinders are usually thin walled open cross sections such as T, Z, L or flat bar sections.

It is well known that if a section has an enforced center of rotation, (i.e. it is not free to twist about its shear center, as a stiffener welded to a shell is not), there is an increase in the warping resistance of the section to torsion (13, 22). For certain cases, it has been shown that the stresses resulting from resistance to warping can have considerable effect on member response and stability (12, 13, 23). In addition, experiments (7, 8, 19) have clearly indicated that importance of stiffener tripping (lateral-torsional instability) as a critical failure mode for ship structures. Hence, it becomes desirable to consider restrained warping stresses in the development of an elasto-plastic stiffener for inclusion in the analysis of stiffened cylinders.

The inclusion of warping stresses in the elastic response of thin walled open cross sections has been studied by many authors in great detail (13, 14, 22). The plastic response of the section under combined stresses is defined by a yield surface. Following procedures suggested by Hodge (16), Morris and Fenves (19) have determined an approximate lower bound to the exact yield surface for a variety of cross sectional types. This investigation included Saint Venant torsion but neglected warping restraint. Boulton (5), Dinno (9, 10) and Gjelsvik (13) have studied the effect of warping restraint on plastic collapse of thin walled open cross sections, but only for simplified cases in which one or more of the possible stress resultants are zero.

This report presents the formulation of an elasto-plastic thin walled open cross section when the effect of warping torsion is more important than Saint Venant torsion. Equations are developed for the yield surface of a Z-section in terms of four stress resultants, namely the axial force, bending moments in two planes, and the warping moment. These are shown to satisfy both upper and lower bound theorems of plasticity and therefore correspond to exact yield surfaces within the assumptions of thin walled sections.

The development of a yield surface including warping restraint is a necessary first step in the analysis of inelastic stiffener tripping. The equations are currently being incorporated into the computer program EPSA (2), developed at Weidlinger Associates under DNA/ONR sponsorship. This implementation is aimed at extending the modeling capability of EPSA to include stiffener tripping and improving structural response predictions in critical regions of large strain and deformation. This capability will be required in the analysis of a series of plastic range tests on both torpedo (7) and submarine scaled model (8) structures.

## KINEMATICS OF THIN WALLED OPEN CROSS SECTIONS

The assumptions made in the formulation of the theory of thin walled beams are that cross sections deform as rigid bodies, and that the shear strain at the middle surface of the section is zero (13, 22).

Referring to Fig. 1, the axial displacement of a point on the middle surface of the bar,  $w(s, z)$ , may be written as (13),

$$w(s, z) = W(z) - U'(z) x(s) - V'(z) y(s) - \phi'(z) \omega(s) \quad (1)$$

where  $\bar{n}$ - $s$ - $z$  are coordinates with  $\bar{n}$  normal to, and  $s$  following the contour of the middle surface;  $U(z)$ ,  $V(z)$ ,  $W(z)$  represent the translation of the center of rotation P in the  $x$ - $y$ - $z$  coordinate system;  $\phi(z)$  is the rotation of the section about the pole P;  $\omega(s)$  is the warping function defined as

$$\omega(s) = \int_0^s r(s) ds \quad (2)$$

where  $r(s)$  is the perpendicular distance from the point P to the point in question on the middle surface. Thickness or secondary warping is neglected in Equation 2.

The first three terms on the right hand side of Equation 1 satisfy Navier's assumption while the last term represents warping.

### Stress and Strain Components

The only non-zero stress components are the longitudinal stress,  $\sigma_{zz}$ , and the shearing stress,  $\tau_{zs}$ , shown in Fig. 2. All stress and strain components normal to the wall are neglected. In addition, all in-plane strains are assumed small. From Eq. 1, the longitudinal strain

is

$$\varepsilon_{zz}(s, z) = W'(z) - U''(z)x(s) - V''(z)y(s) - \phi''(z)\omega(s) \quad (3)$$

If it is desired to extend this formulation to account for geometric nonlinearities, the appropriate nonlinear strain-displacement relations would have to be introduced. This has been done in (6).

#### Stress Resultants

The strain energy per unit length of the bar,  $U_s$ , can be expressed as (13),

$$2U_s = NW' + M_y U'' - M_x V'' + M_\omega \phi'' + T_s \phi' \quad (4)$$

In Eq. 4, the stress resultants  $N$ ,  $M_y$ , and  $M_x$  represent the axial force and bending moments about the  $y$ -axis and  $x$ -axis, respectively, Saint Venant torque is denoted by  $T_s$ , and  $M_\omega$  is the warping moment or bimoment, and is defined as

$$M_\omega = - \int_A \sigma_{zz} \omega \, dA \quad (5)$$

These stress resultants are shown in Fig. 3.

### DECOUPLING OF THE MIXED TORSION PROBLEM

The last two terms of the right hand side of Eq. 4 are the contribution of the warping moment and Saint Venant torsion to the strain energy of the bar. In certain applications, effects of one of these may predominate. In the elastic range, the relative importance of Saint Venant torsion to the warping torsion in straight beams is given by the magnitude of a dimensionless bar parameter,  $\mu_L$ , defined in (13) as

$$\mu_L = L/d \quad (6)$$

in which  $L$  is the span length of the bar and  $d$  is a characteristic length defined by

$$d^2 = EI_{\omega\omega} / GJ \quad (7)$$

where  $E$  and  $G$  denote Young's modulus and the shear modulus and  $I_{\omega\omega}$  and  $J$  are the warping constant and torsion constant.

It has been shown, (13 , 22), that when  $\mu_L$  is small (approximately 1) warping torsion is dominant and the Saint Venant torsion term in Eq. 4 may be neglected. If  $\mu_L$  is large (approximately 20), Saint Venant torsion controls and the term containing the warping moment in Eq. 4 may be dropped.

In the plastic range, the relative importance of these two effects may be estimated by using Eq. 6 with  $d$  assumed equal to its elastic value and  $L$  taken as an effective length corresponding to plastic deformation patterns of the bar.

### Case Study

The preceding discussion on approximations to the mixed torsion problem is applied to a typical problem of interest. Consider the

ring-stiffened cylinder in Fig. 4. A cross section of a typical stiffener is also shown. The value for the warping constant,  $I_{\omega\omega}$ , for the Z-stiffener with an enforced center of rotation about the line of attachment between the stiffener and the shell is  $.0176 \text{ in}^6$  ( $4.73 \times 10^6 \text{ mm}^6$ ). The value of the torsional constant,  $J$ , is  $.00253 \text{ in}^4$  ( $1053 \text{ mm}^4$ ), (14, 15). Using a value for  $E/G = 2.6$  for the steel structure,  $d^2$  given by Eq. 7 is  $18 \text{ in}^2$  ( $11610 \text{ mm}^2$ ).

It has been shown experimentally and analytically in (4, 18) that for cylinders with relatively stiff ring-stiffeners, plastic deformational patterns are characterized by a large number of circumferential waves (typically greater than five). A conservative estimate of an upper bound to the effective length of the ring-stiffener may therefore be taken to be that corresponding to the  $n = 5$  deformational mode. The resulting value of  $\mu_L$  should also be an upper bound. The effective length is then one-tenth of the ring circumference. Using a value of  $8.9 \text{ in}$  ( $226 \text{ mm}$ ) for the length of the stiffener, a value of  $\mu_L = 2$  is obtained. With this value of  $\mu_L$  as an upper bound, Saint Venant torsion may be neglected in Eq. 4, and only the four stress resultants contributing to the axial stress,  $\sigma_{zz}$ , need be considered.

## PLASTIC BEHAVIOR

In the formulation of a plastic theory of thin walled bars, the assumption is made that the kinematics describing the plastic behavior of the bar are the same as in the elastic range, (13).

The plastic response of a bar is defined by a yield surface. The assumptions made in the derivation of this surface, in addition to the kinematic ones are the following:

- 1) the material is elastic-perfectly plastic,
- 2) the von Mises yield condition applies,
- 3) shear stresses due to warping are ignored as in plastic beam theory, (20),
- 4) the yield surface is a closed, convex surface and the incremental plastic deformation is directed outward, normal to the surface. With these assumptions, Drucker's hypotheses, (11), are satisfied insuring both uniqueness and stability of plastic response.

The validity of any proposed yield surface may be assessed using the upper and lower bound theorems of plastic analysis, (20). The lower bound theorem states that if a yield surface is derived from a safe and statically admissible stress state it will be enclosed by or coincide with the correct yield surface. The upper bound theorem states that if the states of stress on a yield surface correspond to assumed mechanisms, that yield surface encloses or coincides with the correct yield surface. These theorems may be combined to form a uniqueness theorem which states that a yield surface, derived from a

safe and statically admissible stress state, and corresponding to a kinematically admissible mechanism, is the one correct yield surface.

The yield condition, formulated in terms of normalized stress resultants, involves only those stress resultants which are contained in the expression for the strain energy, (16). Referring to the previous discussion on approximations in the mixed torsion problem, it is assumed that the effects of Saint Venant torsion are negligible. The strain energy of the bar,  $U_s$ , of Eq. 4, reduces to

$$2U_s = NW' + M_y U'' - M_x V'' + M_\omega \phi'' \quad (8)$$

Hence, the yield condition may be expressed in terms of the dimensionless parameters

$$n = N/N_p \quad (9a)$$

$$m_x = M_x/M_{xp} \quad (9b)$$

$$m_y = M_y/M_{yp} \quad (9c)$$

$$m_\omega = M_\omega/M_{wp} \quad (9d)$$

in which  $N$ ,  $M_x$ ,  $M_y$ , and  $M_\omega$  are the previously defined stress resultants shown in Fig. 3 and  $N_p$ ,  $M_{xp}$ ,  $M_{yp}$ ,  $M_{wp}$  are their fully plastic values. Since shear stresses have been neglected, the von Mises yield condition reduces to

$$\sigma_{zz}^2 = \sigma_y^2 \quad (10)$$

in which  $\sigma_y$  is the yield stress of the material under uniaxial stress.

### DETERMINATION OF A LOWER BOUND YIELD SURFACE

It is evident from Eq. 1 that, if warping is considered, Navier's hypothesis is not valid for the cross section as a whole. It is assumed, however, that Navier's hypothesis does hold for each element of the cross section. This implies that there is one neutral axis contained in each element of the cross section.

The equations for the yield surface may be simplified by the following approximations for thin walled sections (19);

- 1) the neutral axis passes perpendicularly through any element of the section, as shown in Fig. 5, or,
- 2) if the neutral axis lies wholly within an element, it is parallel to the long dimension of the element, Fig. 5.

To illustrate the derivation of yield surface equations for a thin walled open cross section including warping stresses, consider the Z-section in Fig. 6. The dimensions of the section which has an enforced center of rotation at P are:

b = width of the flanges;

h = depth of section, center to center of the flanges;

$A_f$  = area of one flange;  $A_w$  = area of web;

t = thickness of web and flanges;  $c = A_w/A_f = h/b$ ;

$\bar{h}$  = distance from P to center of top flange where typically  $h/\bar{h} \approx 1$ .

The fully plastic stress resultants are found to be:

$$N_p = \sigma_y A_f (2 + c) \quad (11a)$$

$$M_{xp} = \frac{1}{4} \sigma_y A_f h (4 + c) \quad (11b)$$

$$M_{yp} = \sigma_y A_f b \quad (11c)$$

$$M_{wp} = \frac{1}{2} \sigma_y A_f b \bar{h} \quad (11d)$$

In general, a yield surface has several elements each related to generic neutral axis positions. The approximations regarding neutral axis location within an element allow a reduction in the number of surface elements comprising the yield surface of a Z-section to four. They are shown in Fig. 7. However, since the section is not symmetric, four complementary cases are necessary for complete determination of the yield surface. In these complementary cases, indicated in Fig. 8, the generic neutral axis locations of Fig. 7 are unchanged but the sign of the yield stress is reversed.

The stress resultants corresponding to the stress distribution of Fig. 9 are:

$$N = \sigma_y A_f (2 + c - 2(\beta + \gamma c + \alpha)) \quad (12a)$$

$$M_x = \sigma_y A_f h (\gamma c(\gamma - 1) - \alpha + \beta) \quad (12b)$$

$$M_y = \sigma_y A_f b (\beta^2 - 2\beta + \alpha^2) \quad (12c)$$

$$M_w = \frac{1}{2} \sigma_y A_f b \bar{h} (1 - 2\alpha^2) \quad (12d)$$

in which  $\alpha$ ,  $\beta$ , and  $\gamma$  are dimensionless parameters that define the neutral axis location in each element of the cross section.

The corresponding normalized stress resultants, found by substituting Eqs. 12 and 11 into Eqs. 9, are:

$$n = 1 - \frac{2(\beta + \gamma c + \alpha)}{2 + c} \quad (13a)$$

$$m_x = \frac{4}{4+c} (\gamma c(\gamma - 1) - \alpha + \beta) \quad (13b)$$

$$m_y = \beta^2 - 2\beta + \alpha^2 \quad (13c)$$

$$m_w = 1 - 2\alpha^2 \quad (13d)$$

Eliminating the parameters  $\alpha$ ,  $\beta$ , and  $\gamma$  from Eqs. 13, the equation of the element of the yield surface for this case is obtained as

$$\begin{aligned} & \left[ \frac{2+c}{2} (1-n) - (1 - \sqrt{\frac{1}{2}(1+m_{\omega}) + m_y} + \sqrt{\frac{1}{2}(1-m_{\omega})}) \right] \\ & \times \left[ \frac{2+c}{2c} (1-n) - \frac{1}{c}(1 - \sqrt{\frac{1}{2}(1-m_{\omega}) + m_y} + \sqrt{\frac{1}{2}(1-m_{\omega})}) - 1 \right] \quad (14) \\ & + 1 - \sqrt{\frac{1}{2}(1+m_{\omega}) + m_y} - \sqrt{\frac{1}{2}(1-m_{\omega})} - \left( \frac{4+c}{4} \right) m_x = 0 \end{aligned}$$

Consider the stress distribution shown in Fig. 10. In this case, a neutral axis lies within the bottom flange. The values of  $n$  and  $m_x$  are insensitive to the angle  $\theta$  since it is necessarily small. The normalized warping moment,  $m_{\omega}$ , is independent of  $\theta$ , and the bending moment about the  $y$ -axis,  $m_y$ , is an unknown function of  $\theta$  and hence indeterminate. The normalized stress resultants are:

$$n = \frac{c + 2(-1 + \beta + \alpha)}{2 + c} \quad (15a)$$

$$m_x = \frac{4(\beta - \alpha)}{4 + c} \quad (15b)$$

$$m_y = \text{indeterminate} \quad (15c)$$

$$m_{\omega} = 1 - 2\alpha^2 \quad (15d)$$

The equation for this element of the yield surface, obtained from Eqs.

15, is independent of  $m_y$  and may be written

$$(2 + c)n + \frac{4 + c}{2} m_x + \sqrt{3(1 - m_{\omega})} + c - 2 = 0 \quad (16)$$

Similarly, equations for the other elements were found. They are shown in tabular form in Figs. 7 and 8. The yield surface constructed from the various surface elements is illustrated in Fig. 11 for the Z-stiffener of Fig. 4. A two dimensional section in the  $n - m_x$  plane is shown for  $m_y = m_{\omega} = 0$ . The range of applicability of each surface

element is indicated on the figure. Isometric plots of the yield surface are shown in Figs. 12 and 13 for  $m_y = 0$  and  $m_u = 0$ , respectively.

### DETERMINATION OF UPPER BOUND - YIELD MECHANISMS - UNIQUENESS

The state of stress in the bar may be expressed in terms of the stress resultants, which may be considered components of a matrix denoted by  $\{Q\}$ :

$$\{Q\} = \{N, M_y, M_x, M_\omega\} \quad (17)$$

The corresponding matrix of bar strains,  $\{q\}$ , is

$$\{q\} = \{W', U'', -V'', \phi''\} \quad (18)$$

The yield surface is a function of the stress resultants such that, at yield,

$$F(N, M_y, M_x, M_\omega) = 0 \quad (19)$$

It has been assumed that the incremental plastic strain is directed outward, normal to the yield surface. This associated flow rule may be stated as

$$\delta q_i = \lambda \frac{\partial F}{\partial Q_i} \quad (20)$$

in which  $\lambda$  is an arbitrary positive proportionality factor and  $\delta q_i$  denotes a component of incremental plastic strain.

From Eq. 20 it follows that the strain increments corresponding to stress points on the yield surface satisfy

$$\frac{\delta q_i}{\delta q_j} = - \frac{\partial Q_j}{\partial Q_i} \quad (21)$$

in which the derivatives on the right hand side are obtained from Eq. 19.

To illustrate the determination of such strain increment rates, consider, e.g., the lower bound stress distribution of Fig. 10. The yield surface equation for this stress state is given by Eq. 16.

The ratios of the components of the plastic strain increments follow from Eqs. 11, 16, and 21. They are

$$-\frac{\delta V''}{\delta W'} = -\frac{\partial N}{\partial M_x} = \frac{2}{cb} \quad (22a)$$

$$\frac{\delta \phi''}{\delta W'} = -\frac{\partial N}{\partial M_\omega} = -\frac{2}{h\alpha b} \quad (22b)$$

$$\frac{\delta U''}{\delta W'} = -\frac{\partial N}{\partial M_y} = 0 \quad (22c)$$

Yield mechanisms may be determined solely from kinematic considerations. Following Eq. 3, the incremental plastic strain may be written as

$$\delta \epsilon_{zz} = -\delta W' \left( -1 + \frac{\delta U''}{\delta W'} x + \frac{\delta V''}{\delta W'} y + \frac{\delta \phi''}{\delta W'} \omega \right) \quad (23)$$

At a neutral axis location in an element of the cross section, the axial strain,  $\epsilon_{zz}$ , and hence,  $\delta \epsilon_{zz}$ , are zero. The neutral axis locations for each surface element are known and indicated in Figs. 7 and 8. Therefore, the components of the yield mechanism may be determined.

Again, consider the stress distribution of Fig. 10. The neutral axis locations and hence the positions at which Eq. 23 equals zero are shown in Table 1. Substitution of the conditions specified in Table 1 into Eq. 23 gives the components of the yield mechanism as follows:

$$-\frac{\delta V''}{\delta W'} = \frac{2}{cb} \quad (24a)$$

$$\frac{\delta \phi''}{\delta W'} = -\frac{2}{h\alpha b} \quad (24b)$$

$$\frac{\delta U''}{\delta W'} = 0 \quad (24c)$$

Comparison of Eqs. 22 and 24 shows that the stress state on this element of the lower bound yield surface corresponds to a yield mechanism. Thus, the uniqueness theorem of plastic analysis is satisfied and the yield surface element, given by Eq. 16, is the correct one.

In a similar manner, the uniqueness theorem can be shown to be satisfied for the remaining surface elements of Figs. 7 and 8. Hence, the complete yield surface, defined by the individual surface elements, is the exact yield surface. The yield mechanisms, derived from kinematics, for each surface element are listed in Table 2.

### ACCURACY AND IMPLEMENTATION OF THE PROPOSED FORMULATION

The accuracy of the proposed formulation rests on two approximations. The first involves the elimination of Saint Venant torsion from the yield condition. The second involves assumptions on neutral axis location within the elements of the cross section.

Referring to the earlier discussion on approximations to the mixed torsion problem, it is evident that as the importance of Saint Venant torsion increases, the proposed formulation will be increasingly in error.

The assumption that a neutral axis passes perpendicularly through an element of the cross section leads to artificial ridges in the yield surface. These ridges lie outside the correct yield surface. This approximation was discussed in detail in (19), and has been shown to be negligible in elasto-plastic analysis of thin walled sections.

The technique used in the development of the yield surface for a Z-section including warping stresses can be applied to any thin-walled open cross section. Other common types used as ring-stiffeners for cylindrical shells are T and L sections.

The proposed yield surface equations are suitable for incorporation into the existing nonlinear, elasto-plastic finite element program, EPSA (2). The present stiffener formulation in the code accounts for plastic response in terms of only two stress resultants, namely the axial force and bending moment about the strong axis of the stiffener. The proposed formulation will extend the structural modeling capability for the class of problems such as that shown

in Fig. 4, and lead to an increase in the accuracy of structural response predictions, especially in regions of large plastic strain and deformation.

#### CONCLUSION

A procedure has been described for deriving yield surface equations for thin-walled open cross sections with an enforced center of rotation for cases in which Saint Venant torsion is small compared to warping torsion. Equations have been derived for the specific case of a Z-section. These equations have been shown to satisfy the uniqueness theorem of plastic analysis thereby furnishing the correct yield surface within the limits of validity of the assumptions made. The applicability and accuracy of the proposed equations are indicated.

#### REFERENCES

- (1) Almroth, B.O., Brogan, F.A., and Stanley, G.M., "Structural Analysis of General Shells, Volume II, User Instructions for STAGSC," LMSC-D633873, Lockheed Palo Alto Research Laboratory, Palo Alto, California, January 1979.
- (2) Atkatsh, R., and Daddazio, R.P., "Dynamic Elasto-Plastic Response of Shells in an Acoustic Medium User's Manual for the EPSA Code," Technical Report No. 27, ONR Contract No. N00014-78-C-0820, Weidlinger Associates, New York, New York, March 1980.
- (3) Bathe, K.J., "ADINA - A Finite Element Program for Automatic Dynamic Incremental Nonlinear Analysis," Rep. No. 82448-1, Massachusetts Institute of Technology, Cambridge, Massachusetts, September 1975, (rev. Dec. 1978).
- (4) Boichot, L. and Reynolds, T.E., "Inelastic Buckling Tests of Ring-Stiffened Cylinders under Hydrostatic Pressure," David Taylor Model Basin, Washington, D.C., Report 1992, 1965.
- (5) Boulton, N.S., "Plastic Twisting and Bending of an I-Beam in which the Warp is Restricted," Int. J. Mech. Sci., Vol. 4, pp. 491-502, Pergamon Press, 1964.
- (6) Connor, J.J., "Analysis of Structural Member Systems," The Ronald Press Company, New York, 1976.
- (7) Daddazio, R., Atkatsh, R., Baron, M.L. and Bieniek, M.P., "Dynamic Elasto-Plastic Response of Mark 37 Torpedo Afterbodies, EPSA Code Comparisons with Experimental Data (U)," Technical Report, Confidential, Defense Nuclear Agency, Contract No. DNA001-79-C-0078, Weidlinger Associates, New York, New York, January 1980.
- (8) Daddazio, R., Atkatsh, R., Baron, M.L. and Bieniek, M.P., "Intermediate Scale Models Subjected to Simulated Nuclear Loading - EPSA Code Comparisons with ISM-A3/A4 Experimental Data and Implications of the ISM-A3/A4 Test Series (U)," Technical Report, Confidential, Defense Nuclear Agency, Contract No. DNA001-79-C-0078, Weidlinger Associates, New York, New York, January 1981.
- (9) Dinno, K.S., and Gill, S.S., "The Plastic Torsion of I-Sections with Warping Restraint," Int. J. Mech. Sci., Vol. 6, pp. 27-43, Pergamon Press, 1964.
- (10) Dinno, K.S., and Merchant, W., "A Procedure for Calculating the Plastic Collapse of I-Sections under Bending and Torsion," The Structural Engineer, Vol. 43, No. 7, July, 1965, pp. 219-221.

- (11) Drucker, D., "On Uniqueness in the Theory of Plasticity," *Q. Appl. Math.*, Vol. 14, pp. 35-42, 1956.
- (12) Ettonney, M.M., and Kirby, J.B., "Warping Restraint in Three-Dimensional Frames," *Journal of the Structural Division, ASCE*, Vol. 107, No. St. 8, Proc. Paper 16475, August, 1981, pp. 1643-1656.
- (13) Gjelsvik, A., "The Theory of Thin Walled Bars," John Wiley & Sons, Inc., New York, New York, 1981.
- (14) Heins, C.P., "Bending and Torsional Design in Structural Members," Lexington Books, Lexington, Massachusetts, 1975.
- (15) Heins, C.P., and Wang, R.C., "Torsional Properties of Open Cross Sections," *Computers & Structures*, Vol. 9, pp. 495-500, Pergamon Press, 1978.
- (16) Hodge, P., "Plastic Analysis of Structures," McGraw-Hill Book Company, Inc., New York, 1959.
- (17) Hodge, P.G. and Sankaranaraya, R., "The Determination of Safe Loads of Beams Subjected to Combined Twisting and Biaxial Bending Moments," *Journal of Applied Mechanics.*, Vol. 26, Trans. ASME, Series E, Number 3, September, 1959, pp. 442-447.
- (18) Lee, L., "General Elastic-Plastic Instability of Ring-Stiffened Cylindrical Shells Under External Pressure," Technical Report No. SM156, ONR Contract No. N00014-67-A-0242-006, University of Notre Dame, Notre Dame, Indiana, February 1973.
- (19) Morris, G.A., and Fenves, S.J., "Approximate Yield Surface Equations," *Journal of the Engineering Mechanics Division, ASCE*, Vol. 95, No. EM 4, Proc. Paper 6741, August, 1969, pp. 937-954.
- (20) Neal, B.G., "The Plastic Methods of Structural Analysis," John Wiley & Sons, Inc., New York, 1963.
- (21) Smith, C.S., "Compressive Strength of Welded Steel Ship Grillages," *Journal of the Royal Institute of Naval Architects*, No. 4 (Oct 1975).
- (22) Vlasov, V.A., "Thin Walled Elastic Beams," translated from Russian, published for the National Science Foundation, Washington, D.C., and the U.S. Department of Commerce by the Israel Program for Scientific Translations, Jerusalem, 1961.
- (23) Yoo, C.H., "Bimoment Contribution to Stability of Thin-Walled Assemblages," *Computers & Structures*, Vol. 11, pp. 465-471, Pergamon Press, 1980.

## NOTATION

The following symbols are used in this paper:

$A_f$ =	cross sectional area of flange;
$b$ =	width of flange;
$c$ =	ratio of area of web to area of flange;
$d$ =	characteristic length;
$E$ =	Young's modulus;
$F$ =	function defining yield surface
$G$ =	shear modulus
$h$ =	depth of section center to center of flanges;
$\bar{h}$ =	distance from pole to center of top flange;
$I_{\omega}$ =	warping constant;
$J$ =	torsion constant;
$L$ =	length of bar;
$M_x$ =	bending moment about x-axis;
$m_x$ =	normalized bending moment about x-axis;
$M_{xp}$ =	fully plastic bending moment about x-axis;
$M_y$ =	bending moment about y-axis;
$m_y$ =	normalized bending moment about y-axis;
$M_{yp}$ =	fully plastic bending moment about y-axis;
$M_{\omega}$ =	warping moment;
$m_{\omega}$ =	normalized warping moment;
$M_{\omega p}$ =	fully plastic warping moment;
$N$ =	axial force;
$n$ =	normalized axial force;
$N_p$ =	fully plastic axial force;
$\bar{n}-s-z$ =	coordinate system defined at middle surface of cross section;
$P$ =	pole or center of rotation;
$Q$ =	matrix of stress resultants;
$q$ =	matrix of bar strains;
$r$ =	perpendicular distance from pole to point on middle surface of section;
$T_s$ =	Saint Venant torque;
$t$ =	thickness of wall of cross section
$U, V, W,$ =	rigid body displacement of pole in the x,y,z, directions;
$U_s$ =	strain energy per unit length of bar;
$w$ =	axial displacement of point on the middle surface of the cross section
$x, y, z$ =	cartesian coordinates;
$\alpha, \beta, \gamma$ =	dimensionless parameters locating neutral axis in cross section;
$\delta q_i$ =	increment of plastic bar strain;

$\varepsilon_{zz}$  = axial strain in section;  
 $\theta$  = orientation of neutral axis in element of cross section;  
 $\lambda$  = positive constant;  
 $\lambda_L$  = dimensionless bar parameter  
 $\sigma_y$  = yield stress of material;  
 $\sigma_{zz}$  = axial stress in section;  
 $\tau_{zs}$  = shear stress in section  
 $\phi$  = rotation of cross section about pole;  
 $\omega$  = contour warping function

Superscript

' = differentiation with respect to z-axis

TABLE 1 - LOCATION OF NEUTRAL AXES FOR SURFACE ELEMENT 2

ELEMENT	x	y	$\omega$
TOP FLANGE	$\alpha b$	$\frac{1}{2} h$	$-hab$
WEB	0	$-\frac{1}{2} h$	0
BOTTOM FLANGE	$-b \leq x \leq 0$	$-\frac{1}{2} h$	0

TABLE 2 - YIELD MECHANISMS

SURFACE ELEMENT	$\delta W'/\delta \phi''$	$\delta U''/\delta \phi''$	$-\delta V''/\delta \phi''$
1	$\frac{\alpha(1-\beta)(1-2\gamma)hb}{2[\alpha+\gamma(1-\beta-\alpha)]}$	$\frac{\alpha(1-\gamma)h}{[\alpha+\gamma(1-\beta-\alpha)]}$	$\frac{-\beta(1-\alpha)b}{[\beta-\gamma(1-\beta-\alpha)]}$
2	$-\frac{1}{2} h\alpha b$	0	$-\alpha b$
3	$-\frac{1}{2} \beta hb$	h	$\beta b$
4	0	h	0
1a	$\frac{\beta(1-\alpha)(2\gamma-1)hb}{2[\beta-\gamma(1-\beta-\alpha)]}$	$\frac{-\gamma(1-\alpha)h}{[\beta-\gamma(1+\beta-\alpha)]}$	$\frac{-\alpha(1-\beta)b}{[\alpha+\gamma(1-\beta-\alpha)]}$
2a	$-\frac{1}{2} h (1-\alpha)b$	0	$-(1-\alpha)b$
3a	$-\frac{1}{2} h (1-\beta)b$	h	$(1-\beta)b$
4a	0	h	0

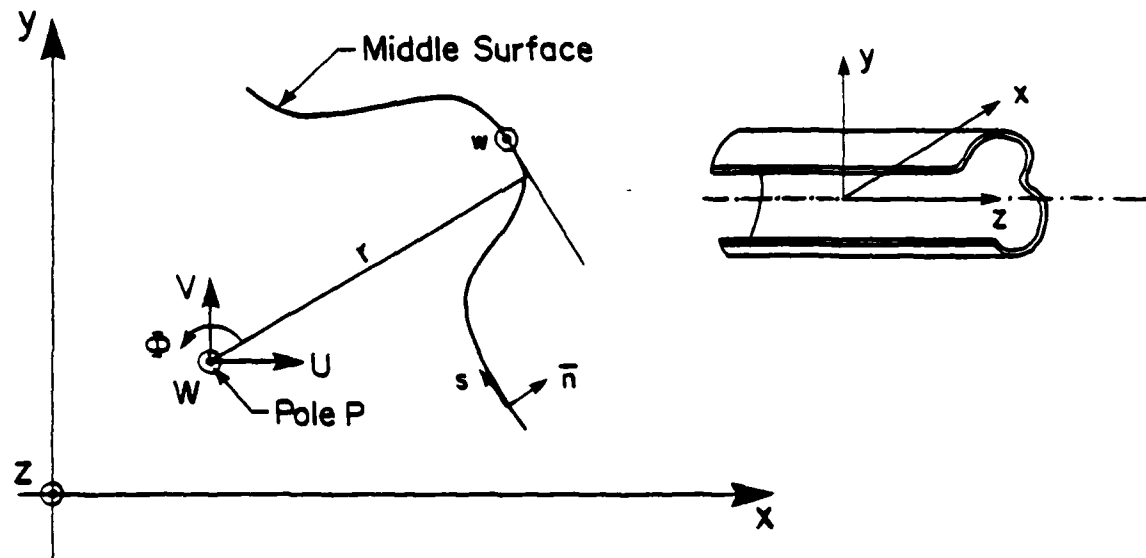


FIG.1 CROSS SECTION DISPLACEMENTS

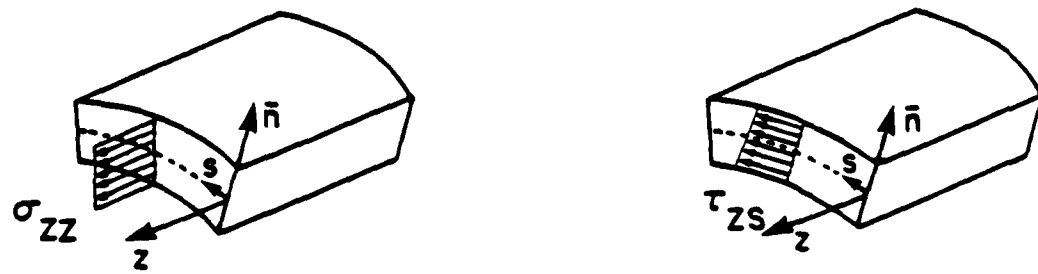


FIG.2 STRESS COMPONENTS

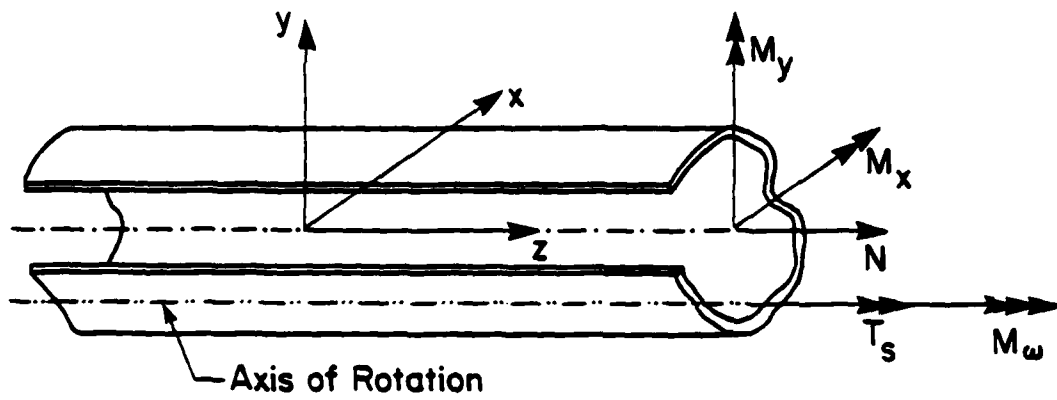


FIG. 3 STRESS RESULTANTS

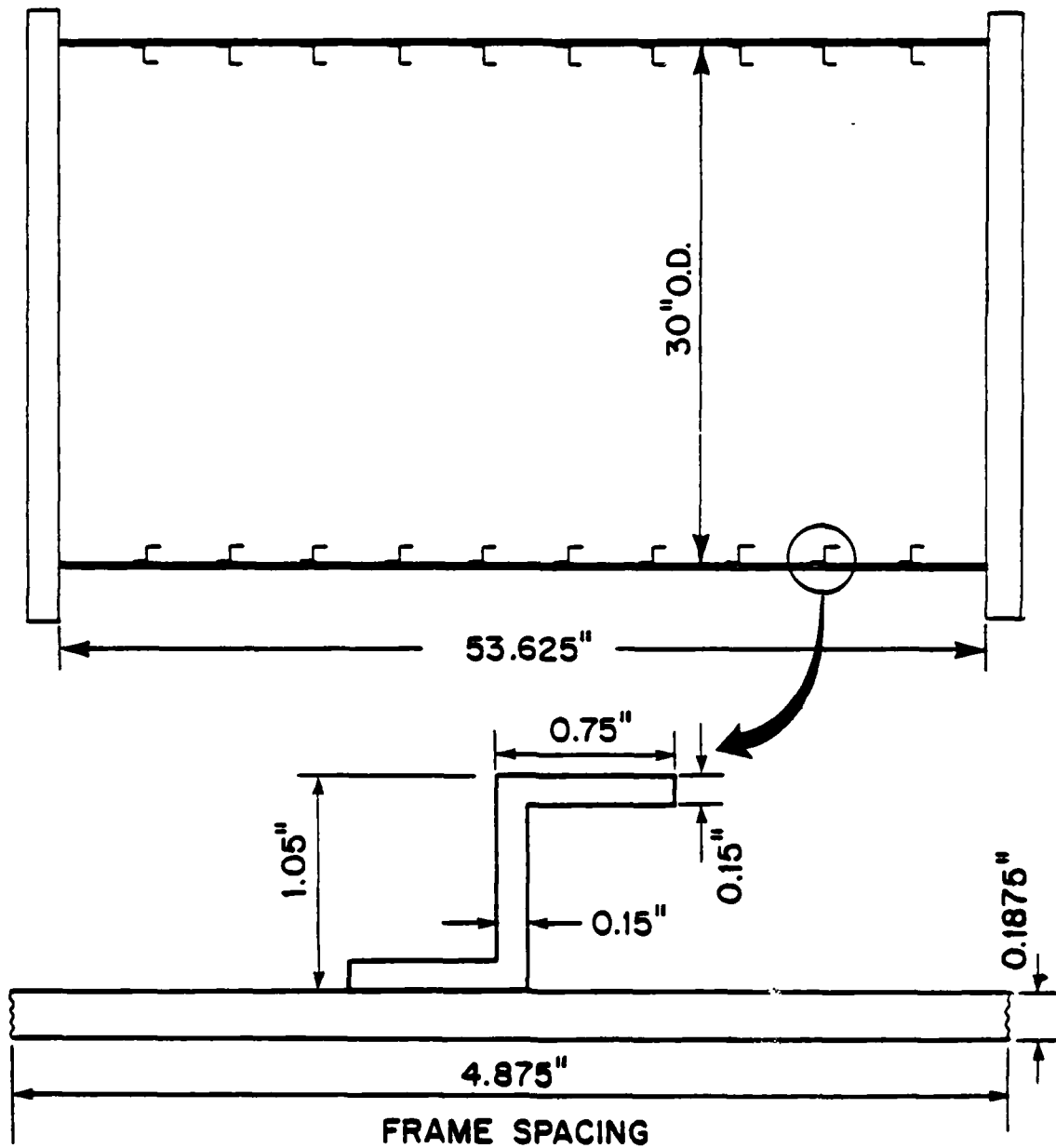


FIG. 4 Z STIFFENED CYLINDRICAL SHELL (1in = 25.4 mm)

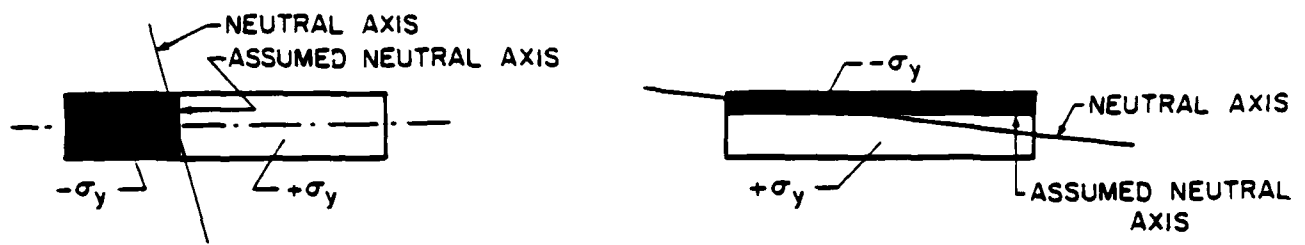


FIG. 5 ASSUMED NORMAL STRESS DISTRIBUTIONS

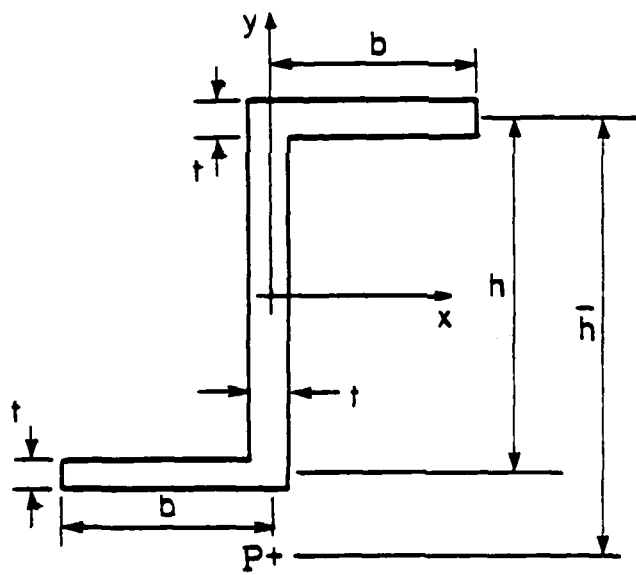


FIG. 6 Z SECTION

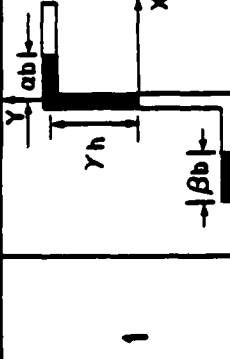
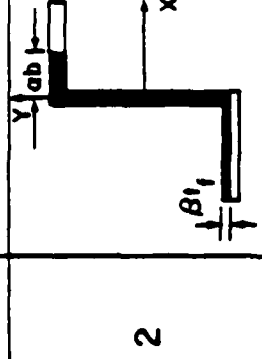
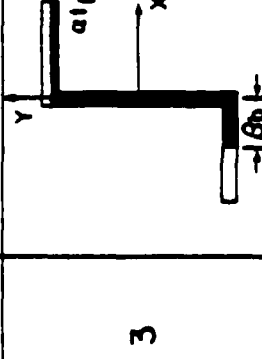
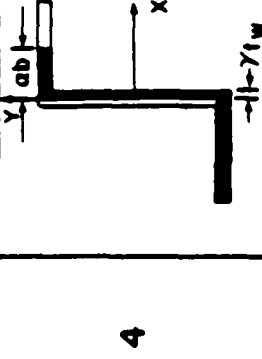
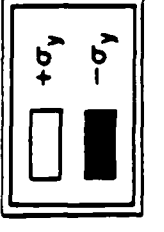
SURFACE ELEMENT	NEUTRAL AXES LOCATION	NORMALIZED STRESS RESULTANTS	YIELD SURFACE EQUATIONS
1		$n = 1 - \frac{2(\beta + \gamma c + a)}{2+c}$ $m_x = \frac{4}{4+c} \left[ \gamma c (\gamma - 1) - a + \beta \right]$ $m_y = \beta^2 - 2\beta + a^2$ $m_\omega = 1 - 2a^2$	$\left[ \left( \frac{2+c}{2} \right) (1-n) - (1 - \sqrt{\frac{1}{2} (1+m_\omega)} + m_y + \sqrt{\frac{1}{2} (1-m_\omega)}) \right] + 1$ $\left[ \left( \frac{2+c}{2c} \right) (1-n) - \frac{1}{c} (1 - \sqrt{\frac{1}{2} (1+m_\omega)} + m_y + \sqrt{\frac{1}{2} (1-m_\omega)}) - 1 \right] + 1$ $- \sqrt{\frac{1}{2} (1+m_\omega)} + m_y - \sqrt{\frac{1}{2} (1-m_\omega)} - \left( \frac{4+c}{4} \right) m_x = 0$
2		$n = - \frac{c+2(-1+\beta+a)}{2+c}$ $m_x = \frac{4(\beta-a)}{(4+c)}$ $m_y = \text{indeterminate}$ $m_\omega = 1 - 2a^2$	$(2+c)n + \frac{4+c}{2} m_x + \sqrt{8(1-m_\omega)} + c - 2 = 0$
3		$n = - \frac{c+2(-1+\beta+a)}{2+c}$ $m_x = \frac{4(\beta-a)}{(4+c)}$ $m_y = \text{indeterminate}$ $m_\omega = \text{indeterminate}$ $\beta = \sqrt{\frac{1}{2} (1-m_\omega)} - m_y$	$-(2+c)n + \frac{4+c}{2} m_x - 4 \sqrt{\frac{1}{2} (1-m_\omega)} - m_y - c + 2 = 0$
4		$n = \text{indeterminate}$ $m_x = \text{indeterminate}$ $m_y = a^2 - 1$ $m_\omega = 1 - 2a^2$	$m_\omega + 2m_y + 1 = 0$ 

FIG. 7 YIELD SURFACE EQUATIONS

SURFACE ELEMENT	NEUTRAL AXES LOCATION	NORMALIZED STRESS RESULTANTS	YIELD SURFACE EQUATIONS
1a		$m_x = \frac{4}{4+c} \left[ \gamma c (1-\gamma) - \alpha + \beta \right]$ $m_y = -\alpha^2 + 2\alpha - \beta^2$ $m_\omega = 1 - 2\alpha(2-\alpha)$	$n = 1 - \frac{2(\beta+\gamma c+\alpha)}{2+c}$ $\left[ \left( \frac{2+c}{2} \right) (1-n) - \sqrt{\frac{1}{2} (1+m_\omega)} - m_y + 1 \sqrt{\frac{1}{2} (1+m_\omega)} \right] +$ $\left[ \left( \frac{2+c}{2c} \right) (1-n) - \frac{1}{c} \left( \sqrt{\frac{1}{2} (1+m_\omega)} - m_y + 1 \sqrt{\frac{1}{2} (1+m_\omega)} \right) - 1 \right] +$ $\sqrt{\frac{1}{2} (1+m_\omega)} - m_y - 1 + \sqrt{\frac{1}{2} (1+m_\omega)} - \left( \frac{4+c}{4} \right) m_x = 0$
2a		$m_x = \frac{4}{4+c} (\beta-\alpha)$ $m_y = \text{indeterminate}$	$n = 1 - \frac{2(\beta+\alpha)}{2+c}$ $(2+c)n + \frac{4+c}{2} m_x - \sqrt{8(1+m_\omega)} - c + 2 = 0$
3a		$m_\omega = 1 - 2\alpha(2-\alpha)$	$n = 1 - \frac{2(\beta+\alpha)}{2+c}$ $m_x = \frac{4}{4+c} (\beta-\alpha)$ $m_y = \text{indeterminate}$ $m_\omega = \text{indeterminate}$ $\beta = 1 - \sqrt{\frac{1}{2} (1+m_\omega)} + m_y$
4a		$m_\omega = \text{indeterminate}$	 $m_\omega + 2m_y - 1 = 0$ $m_y = \alpha^2 + 2\alpha - 1$ $m_\omega = 1 - 2\alpha(2-\alpha)$

FIG. 8 YIELD SURFACE EQUATIONS

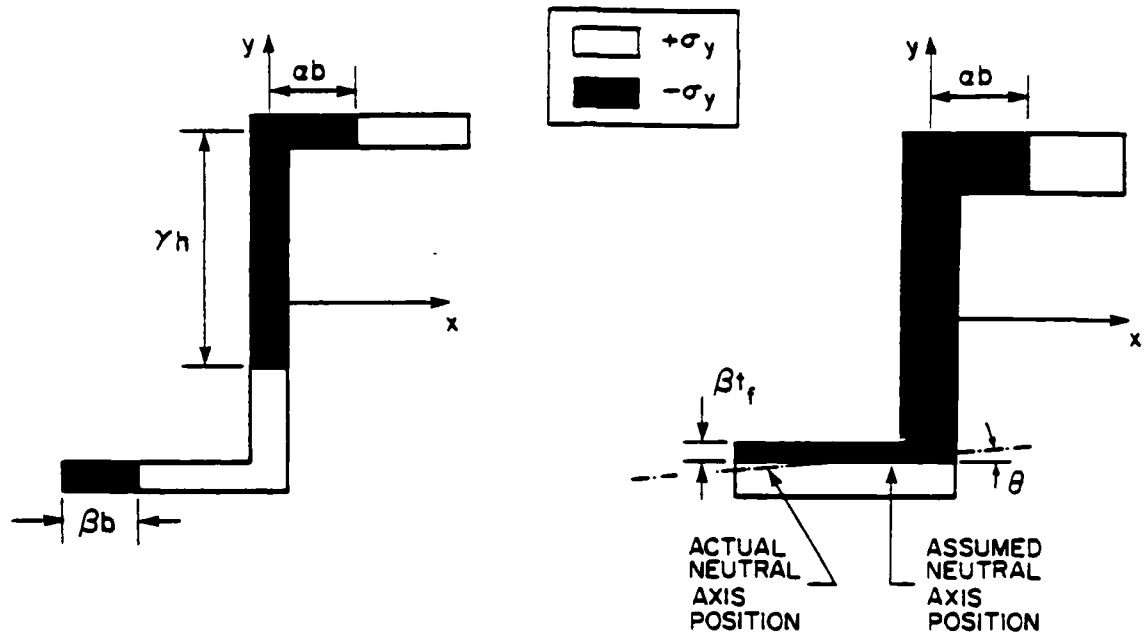


FIG. 9 ASSUMED STRESS DISTRIBUTION FOR SURFACE ELEMENT 1

FIG.10 ASSUMED STRESS DISTRIBUTION FOR SURFACE ELEMENT 2

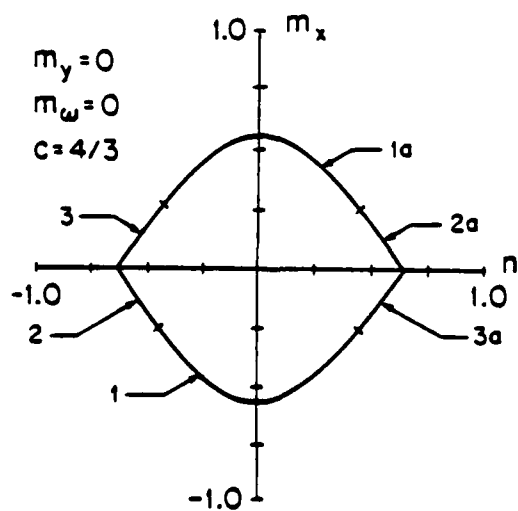


FIG.11 Z SECTION YIELD SURFACE

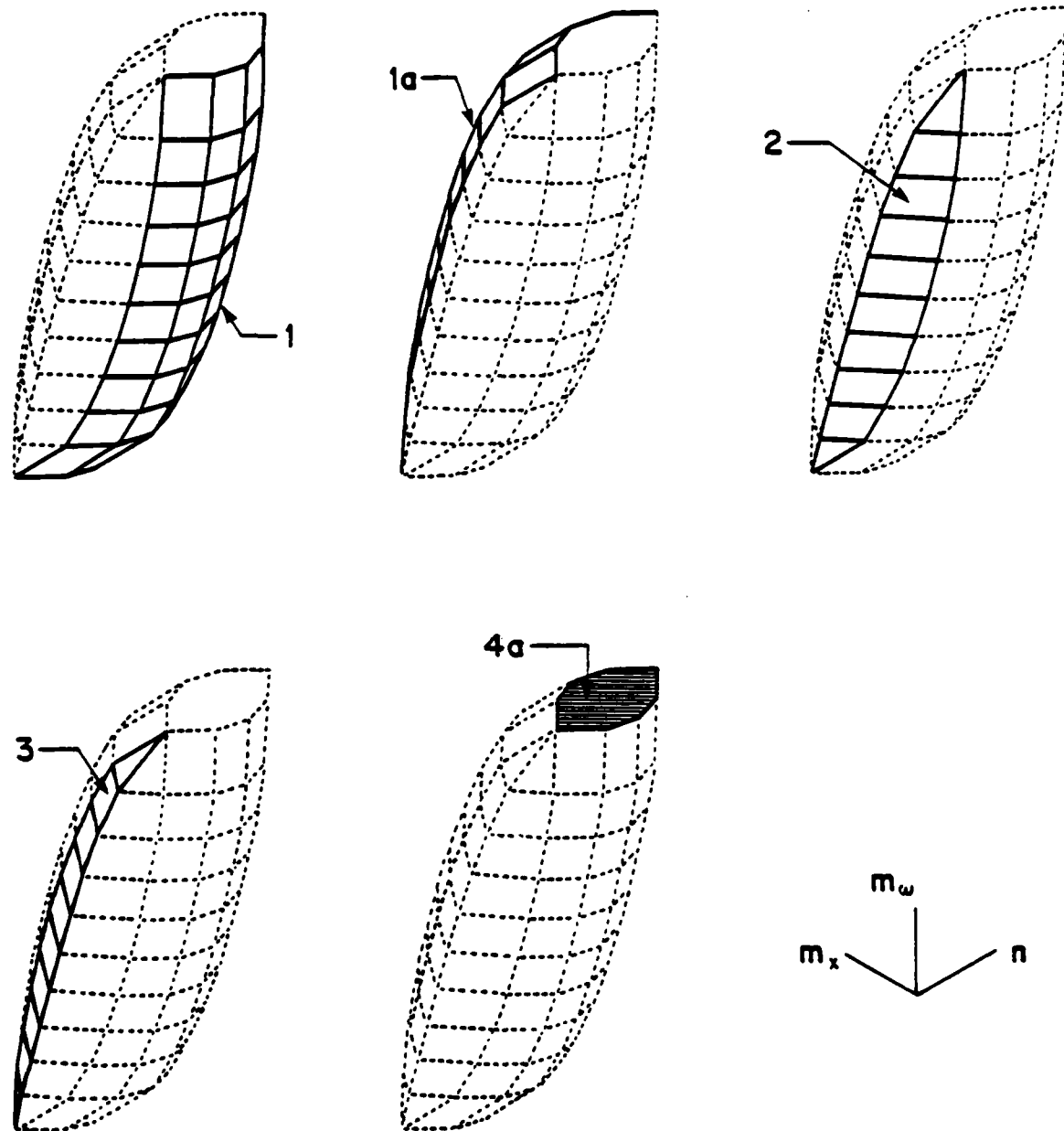


FIG. 12 Z SECTION YIELD SURFACE -  $m_y=0$

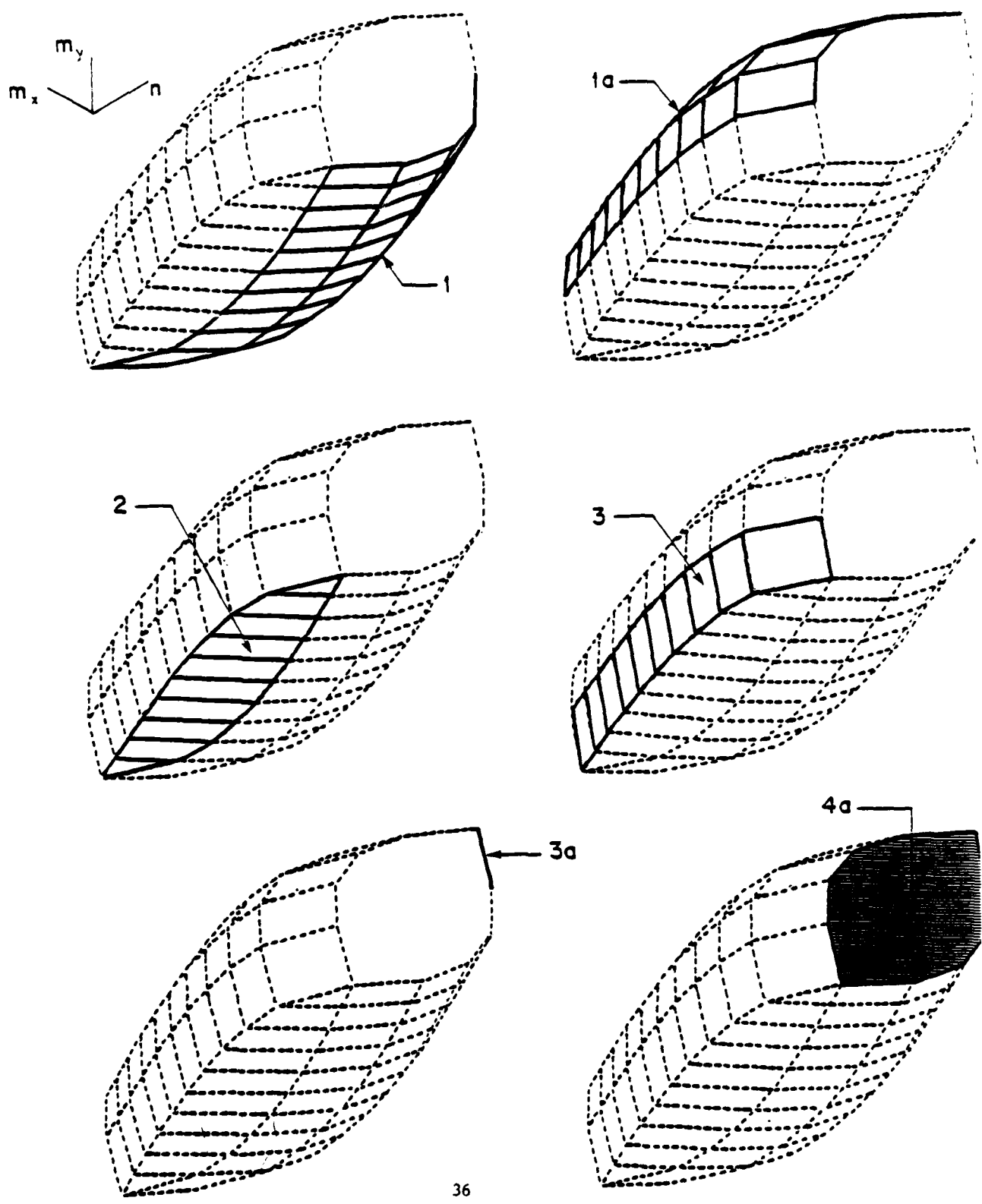


FIG. 13 Z SECTION YIELD SURFACE -  $m_\omega = 0$

## DISTRIBUTION LIST

### DEPARTMENT OF DEFENSE

Assistant to the Secretary of Defense  
 Atomic Energy  
     ATTN: Executive Assistant

Defense Intelligence Agency  
     ATTN: DB-4C2  
     ATTN: DB-4C2, C. Wiegle  
     ATTN: DT-1C  
     ATTN: DT-2  
     ATTN: RTS-2A  
     ATTN: DB-4C3  
     ATTN: DB-4C, Rsch, Phys Vuin Br  
     ATTN: DB-4C1

Defense Nuclear Agency  
     ATTN: SPSS  
     ATTN: STSP  
     4 cy ATTN: TITL

Defense Technical Information Center  
 12 cy ATTN: DD

Field Command  
 Defense Nuclear Agency, Det 1  
 Lawrence Livermore Lab  
     ATTN: FC-1

Field Command  
 Defense Nuclear Agency  
     ATTN: FCPR  
     ATTN: FCT  
     ATTN: FCTX  
     ATTN: FCTT, G. Ganong  
     ATTN: FCTT, W. Summa  
     ATTN: FCTXE

Interservice Nuclear Weapons School  
     ATTN: TTV

Joint Strat Tgt Planning Staff  
     ATTN: NRI-STINFO Library  
     ATTN: JLA, Threat Applications Div  
     ATTN: JLW, R. Autenberg  
     ATTN: JLW-2  
     ATTN: DOXT  
     ATTN: XPFS

Under Secy of Def for Rsch & Engrg  
     ATTN: Strategic & Space Sys (OS)

### DEPARTMENT OF THE ARMY

BMD Advanced Technology Center  
     ATTN: ICRDABH-X  
     ATTN: ATC-T

Chief of Engineers  
     ATTN: DAEN-RDL  
     ATTN: DAEN-MPE-T

Deputy Chief of Staff for Ops & Plans  
     ATTN: DAMO-NC, Nuc Chem Dir

Deputy Chief of Staff for Rsch Dev & Acq  
     ATTN: DAMA

### DEPARTMENT OF THE ARMY (Continued)

Engineer Studies Center  
     ATTN: DAEN-FES, LTC Hatch

Harry Diamond Laboratories  
     ATTN: DELHD-NW-P  
     ATTN: DELHD-TA-L

US Army Concepts Analysis Agency  
     ATTN: CSSA-ADL

US Army Engineer Ctr & Ft Belvoir  
     ATTN: ATZA-DTE-ADM

US Army Engineer School  
     ATTN: ATZA, CDC

US Army Engr Waterways Exper Station  
     ATTN: R. Whalin  
     ATTN: WESSE  
     ATTN: WESSD, J. Jackson  
     ATTN: J. Strange  
     ATTN: J. Zelasko  
     ATTN: F. Brown  
     ATTN: Library  
     ATTN: WESSA, W. Flathau  
     ATTN: WESSS, J. Ballard

US Army Foreign Science & Tech Ctr  
     ATTN: DRXST-SD

US Army Mat Cmd Proj Mngr for Nuc Munitions  
     ATTN: DRCPM-NUC

US Army Material & Mechanics Rsch Ctr  
     ATTN: DRXMR, J. Mescall  
     ATTN: Technical Library

US Army Materiel Dev & Readiness Cmd  
     ATTN: DRCDE-D, L. Flynn  
     ATTN: DRXAM-TL

US Army Nuclear & Chemical Agency  
     ATTN: Library

US Army War College  
     ATTN: Library

USA Military Academy  
     ATTN: Document Library

### DEPARTMENT OF THE NAVY

Marine Corp Dev & Education Command  
     ATTN: D091, J. Hartneady

Marine Corps  
     ATTN: POM

Naval Civil Engineering Laboratory  
     ATTN: Code L51, J. Crawford

Naval Coastal Systems Laboratory  
     ATTN: Code 741

DEPARTMENT OF THE NAVY (Continued)

David Taylor Naval Ship R&D Ctr  
ATTN: Code L42-3  
ATTN: Code 1700, W. Murray  
ATTN: Code 1844  
ATTN: Code 177, E. Palmer  
ATTN: Code 172  
ATTN: Code 1770.1  
ATTN: Code 174  
ATTN: Code 2740  
ATTN: Code 1740.4  
ATTN: Code 1740, R. Short  
ATTN: Code 173  
ATTN: Code 11  
ATTN: Code 1740.5  
ATTN: Code 1740.6  
ATTN: Code 1740.1

Naval Electronic Systems Command  
ATTN: PME 117-21

Naval Explosive Ord Disposal Fac  
ATTN: Code 504, J. Petrousky

Naval Facilities Engineering Command  
ATTN: Code 04B

Naval Material Command  
ATTN: MAT 08T-22

Naval Ocean Systems Center  
ATTN: Code 013, E. Cooper  
ATTN: Code 4471

Naval Postgraduate School  
ATTN: Code 69NE  
ATTN: Code 1424, Library  
ATTN: Code 69SG, Y. Shin

Naval Research Laboratory  
ATTN: Code 8403, R. Belsham  
ATTN: Code 8440, G. O'Hara  
ATTN: Code 6380  
ATTN: Code 8100  
ATTN: Code 8301  
ATTN: Code 8406  
ATTN: Code 2627  
ATTN: Code 8445  
ATTN: Code 8404, H. Pusey

Naval Sea Systems Command  
ATTN: SEA-033  
ATTN: SEA-323  
ATTN: SEA-06J, R. Lane  
ATTN: SEA-09G53  
ATTN: SEA-55X1  
ATTN: SEA-08  
ATTN: SEA-0351  
ATTN: SEA-9931G

Naval Surface Weapons Center  
ATTN: Code F34  
ATTN: Code R13  
ATTN: Code F10  
ATTN: Code U401, M. Kleinerman  
ATTN: Code R14  
ATTN: Code F31  
ATTN: Code R15

DEPARTMENT OF THE NAVY (Continued)

Naval Surface Weapons Center  
ATTN: W. Wishard  
ATTN: Tech Library & Info Svcs Br

Naval War College  
ATTN: Code E-11

Naval Weapons Center  
ATTN: Code 233  
ATTN: Code 266, C. Austin  
ATTN: Code 3263, J. Bowen

Naval Weapons Evaluation Facility  
ATTN: G. Binns  
ATTN: Code 10  
ATTN: Code 210  
ATTN: R. Hughes

Naval Weapons Support Center  
ATTN: Code 70553, D. Moore

New London Laboratory  
ATTN: Code 4494, J. Patel  
ATTN: Code 4492, J. Kalinowski

Newport Laboratory  
ATTN: Code EM  
ATTN: Code 363, P. Paranzino

Ofc of the Deputy Chief of Naval Ops  
ATTN: OP 987  
ATTN: NOP 982, Tac Air Srf & Ewdev Div  
ATTN: NOP 981  
ATTN: NOP 654, Strat Eval & Anal Br  
ATTN: OP 098T8  
ATTN: OP 982E, M. Lenzini  
ATTN: OP 957E  
ATTN: NOP 953, Tac Readiness Div  
ATTN: OP 37  
ATTN: OP 225  
ATTN: OP 03EG  
ATTN: OP 21  
ATTN: NOP 951, ASW Div  
ATTN: OP 605D5  
ATTN: OP 981N1  
ATTN: OP 223

Office of Naval Research  
ATTN: Code 474, N. Perrone

Strategic Systems Project Office  
ATTN: NSP-272  
ATTN: NSP-43  
ATTN: NSP-273

DEPARTMENT OF THE AIR FORCE

Air Force Institute of Technology  
ATTN: Commander  
ATTN: Library

Air Force Systems Command  
ATTN: DLW

Assistant Chief of Staff  
Intelligence  
ATTN: IN

DEPARTMENT OF THE AIR FORCE (Continued)

Air Force Weapons Laboratory  
ATTN: NTES-G, S. Melzer  
ATTN: NTE, M. Plamondon  
ATTN: NTES-C, R. Henny  
ATTN: SUL  
ATTN: NTED

Ballistic Missile Office  
ATTN: DEB

Deputy Chief of Staff  
Research, Development, & Acq  
ATTN: AFROQI  
ATTN: R. Steere

Deputy Chief of Staff  
Logistics & Engineering  
ATTN: LEEE

Foreign Technology Division  
ATTN: NIIS Library  
ATTN: TOTD  
ATTN: SDBG  
ATTN: SDBF, S. Spring

Rome Air Development Center  
ATTN: RBES, R. Mair  
ATTN: Commander  
ATTN: TSLD

Strategic Air Command  
ATTN: NRI-STINFO Library

DEPARTMENT OF ENERGY

Albuquerque Operations Office  
ATTN: CTID

Department of Energy  
ATTN: OMA/RD&T

Nevada Operations Office  
ATTN: Doc Con for Technical Library

OTHER GOVERNMENT AGENCIES

Central Intelligence Agency  
ATTN: OSWR/NED  
ATTN: OSR/SE/F

NASA  
ATTN: F. Nichols  
ATTN: R. Jackson

NATO

NATO School  
SHAPE  
ATTN: US Documents Officer

DEPARTMENT OF ENERGY CONTRACTORS

University of California  
Lawrence Livermore National Lab  
ATTN: S. Erickson

DEPARTMENT OF ENERGY CONTRACTORS (Continued)

Los Alamos National Laboratory  
ATTN: R. Whitaker  
ATTN: MS530, G. Spillman  
ATTN: Reports Library  
ATTN: MS634, T. Dowler  
ATTN: R. Sanford  
ATTN: MS670, J. Hopkins

DEPARTMENT OF DEFENSE CONTRACTORS

Applied Research Associates, Inc  
ATTN: D. Piepenburg

Applied Research Associates, Inc  
ATTN: B. Frank

BDM Corp  
ATTN: T. Neighbors  
ATTN: A. Lavagnino  
ATTN: Corporate Library

California Institute of Technology  
ATTN: T. Ahrens

California Research & Technology, Inc  
ATTN: M. Rosenblatt  
ATTN: S. Schuster  
ATTN: Library  
ATTN: K. Kreyenhagen

Columbia University  
ATTN: H. Bleich  
ATTN: F. Dimaggio

University of Denver  
ATTN: Sec Officer for J. Wisotski

Electric Power Research Institute  
ATTN: G. Sliter

Electro-Mech Systems, Inc  
ATTN: R. Shunk

General Dynamics Corp  
ATTN: J. Miller  
ATTN: J. Mador  
ATTN: M. Pakstys

Kaman AviDyne  
ATTN: R. Ruetenik  
ATTN: G. Zartarian  
ATTN: Library  
ATTN: N. Hobbs

Kaman Sciences Corp  
ATTN: Library  
ATTN: F. Shelton

Kaman Sciences Corp  
ATTN: D. Sachs

Kaman Tempo  
ATTN: DASIAC

DEPARTMENT OF DEFENSE CONTRACTORS (Continued)

Karagozian and Case  
ATTN: J. Karagozian

Lockheed Missiles & Space Co., Inc  
ATTN: Technical Information Center  
ATTN: T. Geers  
ATTN: B. Almroth

Lockheed Missiles & Space Co., Inc  
ATTN: TIC-Library

M & T Company  
ATTN: D. McNaught

Management Science Associates  
ATTN: K. Kaplan

McDonnell Douglas Corp  
ATTN: R. Halprin

NKF Engineering Associates, Inc  
ATTN: R. Belsheim

Pacific-Sierra Research Corp  
ATTN: H. Brode, Chairman SAGE

Pacifica Technology  
ATTN: R. Bjork  
ATTN: G. Kent  
ATTN: A. Kushner

Physics Applications, Inc  
ATTN: C. Vincent

Physics International Co  
ATTN: L. Behrmann  
ATTN: F. Sauer  
ATTN: J. Thomsen  
ATTN: E. Moore  
ATTN: Technical Library

Science Applications, Inc  
ATTN: Technical Library

Southwest Research Institute  
ATTN: A. Wenzel  
ATTN: W. Baker

DEPARTMENT OF DEFENSE CONTRACTORS (Continued)

S-CUBED  
ATTN: T. Cherry  
ATTN: R. Sedgewick  
ATTN: D. Grine  
ATTN: T. Riney  
ATTN: Library  
ATTN: K. Pyatt  
ATTN: T. McKinley

SRI International  
ATTN: G. Abrahamson  
ATTN: W. Wilkinson  
ATTN: A. Florence

Teledyne Brown Engineering  
ATTN: J. Ravenscraft

Tetra Tech, Inc  
ATTN: L. Hwang

TRW Electronics & Defense Sector  
ATTN: P. Bhuta  
ATTN: A. Feldman  
ATTN: N. Lipner  
ATTN: Technical Information Center  
ATTN: D. Jortner  
ATTN: B. Sussholtz

TRW Electronics & Defense Sector  
ATTN: P. Dai  
ATTN: F. Pieper  
ATTN: E. Wong  
ATTN: G. Hulcher

Weidlinger Assoc, Consulting Engrg  
ATTN: J. McCormick  
ATTN: M. Baron  
4 cy ATTN: R. Daddazio  
4 cy ATTN: M. Bieniek  
4 cy ATTN: F. DiMaggio

Weidlinger Associates  
ATTN: J. Isenberg

**DATE  
ILME**